



Cite this: *RSC Adv.*, 2020, 10, 40719

## Refractive index of delignified wood for transparent biocomposites

Hui Chen,<sup>a</sup> Céline Montanari,<sup>a</sup> Max Yan,<sup>b</sup> Sergei Popov,<sup>b</sup> Yuanyuan Li,<sup>\*a</sup> Ilya Sychugov<sup>\*b</sup> and Lars A Berglund<sup>a</sup>

Refractive index (RI) determination for delignified wood templates is vital for transparent wood composite fabrication. Reported RIs in the literature are based on either single plant fibers or wood powder, measured by the immersion liquid method (ILM) combined with mathematical fitting. However, wood structure complexity and the physical background of the fitting were not considered. In this work, RIs of delignified wood templates were measured by the ILM combined with a light transmission model developed from the Fresnel reflection/refraction theory for composite materials. The RIs of delignified balsa wood are  $1.536 \pm 0.006$  and  $1.525 \pm 0.008$  at the wavelength of 589 nm for light propagating perpendicular and parallel to the wood fiber direction, respectively. For delignified birch wood, corresponding values are  $1.537 \pm 0.005$  and  $1.529 \pm 0.006$ , respectively. The RI data for delignified wood scaffolds are important for tailoring optical properties of transparent wood biocomposites, and also vital in optical properties investigations by theoretical modelling of complex light propagation in transparent wood and related composites. The developed light transmission model in combination with the immersion liquid method can be used to determine the RI of complex porous or layered solid materials and composites.

Received 28th August 2020  
Accepted 3rd November 2020

DOI: 10.1039/d0ra07409h

rsc.li/rsc-advances

Wood is traditionally a well-established material in construction. Recently, however, this bio-based material has found a new lease of life in numerous other applications, such as wood packaging materials,<sup>1</sup> sound insulation materials<sup>2</sup> and transparent wood materials.<sup>3,4</sup> In multi-phase composite materials, such as transparent plant fiber composites,<sup>5</sup> knowing the refractive index (RI) of the constituents is crucial for optical property tailoring. To obtain a high optical transmittance in polymer composites, the constituent RIs need to be matched. Transparent wood biocomposites<sup>3,4,6,7</sup> is a good example, where the selection of a suitable polymer relies on an accurate value of RI of the delignified wood template, which is the reinforcing structure of the material. So far, reported RI values for such materials are approximations based on single plant fibers or wood powder, while the complexity of the original wood structure was not taken into account. Wood has a porous and anisotropic structure (Fig. 1) with microscale cell lumen porosity.<sup>8</sup> The large majority of tubular cells are aligned in the axial direction (for example vessels and fibers) although a very small cell fraction is aligned in the perpendicular direction of the tree stem (wood rays).<sup>9</sup> In addition, the delignified wood

template is a mixture of cellulose, hemicelluloses and residual lignin components.<sup>10</sup> Cellulose fiber is a birefringent material due to the orientation of the cellulose molecules and microfibrils.<sup>11</sup> Component composition, microfibril angle (MFA, angle between microfibril and the fiber axis), as well as moisture content varies for different fibers, leading to RI variations.<sup>12–15</sup> Frey reported the influence of MFA on the RIs of cellulose fiber. The measured RI of the fiber corresponds to microfibril orientation and is described by an elliptical formula.<sup>12</sup> The lignin/hemicellulose content influence the RI and the birefringence property of the fiber. Kanamaru reported that with higher

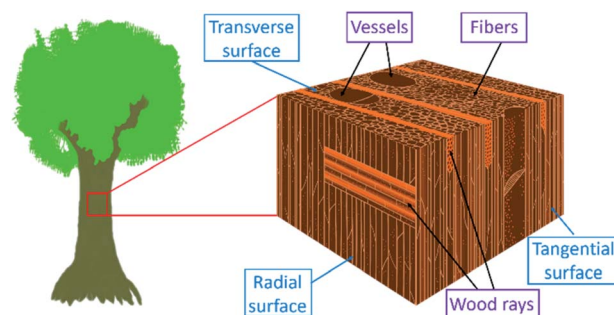


Fig. 1 Microstructure of hardwoods with vessels and fiber cells, as well as ray cells. Typical fiber cell diameter in hardwoods is about 20  $\mu\text{m}$ , with a fiber length of around 1 mm.

<sup>a</sup>Wallenberg Wood Science Center, Department of Fiber and Polymer Technology, KTH Royal Institute of Technology, Teknikringen 56, 10044, Stockholm, Sweden. E-mail: yua@kth.se

<sup>b</sup>Department of Applied Physics, KTH Royal Institute of Technology, Hannes Alfvéns väg 12, 11419, Stockholm, Sweden. E-mail: ilyas@kth.se



cellulose content, the RI parallel to the fiber direction is increased, but it is decreased perpendicular to the fiber direction, so that the birefringence is increased.<sup>14</sup> The moisture content/swelling of the fiber also influence the RI and birefringence. Madeleine and Hermans reported that with increased moisture content, RIs parallel and perpendicular to the fiber direction as well as the birefringence are decreased.<sup>13,15</sup> Thus, an accurate RI measurement technique for delignified wood templates is of basic importance for technical and scientific purposes.

The immersion liquid method, ILM, is a common technique for RI measurements of solid materials,<sup>16</sup> such as minerals,<sup>17</sup> wood powders,<sup>18,19</sup> plastic fibers<sup>20</sup> and turbid media.<sup>21,22</sup> The main principle is to immerse the material in a mixture of two different liquids with different RIs. At a given proportion of the two liquids, the RI of the liquid phase matches the RI of the material of interest. The mixed solid-liquid material then becomes transparent, and the RI of the material is estimated based on the equation:  $RI = (V_a n_a + V_b n_b) / (V_a + V_b)$ , where  $V_a$  and  $n_a$ ,  $V_b$  and  $n_b$  are the volume and the RI of the two liquids, respectively.<sup>18,19</sup> This experimental approach has been applied to cellulose-based materials.<sup>23–25</sup> Preston reports the RI of native cotton and ramie fibers at 589 nm wavelength, measured by ILM. The results for native cotton are 1.532 perpendicular to the fiber direction, and 1.578 parallel to the fiber direction. The values for ramie fiber are 1.528 and 1.596, respectively.<sup>26</sup> Patel reports measurements of ramie fiber RI by immersing the fibers in a series of mixtures. The obtained values are 1.5264 perpendicular to the fiber direction and 1.5969 parallel to the fiber direction at 589 nm.<sup>23</sup> Iyer reports the RI of cellulose nanocrystals by the same technique. RI is 1.603 along the fiber direction and 1.523 perpendicular to the fiber direction.<sup>25</sup> However, this approach is laborious and it is difficult to find the exact RI of the solvent mixture to match RI of the tested material.

To overcome the problems, analytic approaches have been applied previously to determine the RI of a solid material. In these methods, the optical transmittance is measured as a function of the RI of the filling liquid. In order to find the maximum transmittance, which corresponds to the “template” RI, a mathematical fitting procedure has been used, with no connection to the physics of the phenomenon. For example, the RI of cellulose nanocrystals was estimated by combining the Beer-Lambert law and ILM, followed by Lorentz fit of the transmittance.<sup>27</sup> Juttula estimated the RI of softwood powder by Gaussian fitting of the transmittance.<sup>19</sup> In addition, Niskanen estimated the RI of thermally modified Scots pine by Gaussian fitting of the backscattering intensity.<sup>18</sup> In the case of mixtures of two liquids used as the immersion liquid, the miscibility, as well as the different evaporation rates of the two liquids would influence the measurements. Nussbaumer applied a modified ILM where different liquids with different RIs were used, then the Lorentz, Gaussian and polynomial fits of the transmittance were compared to determine the RI of a solid.<sup>28</sup> The drawbacks are that the fittings are typically statistical, again lacking a physical background and interpretation, and the materials structure is not taken into account. If the mathematical fitting

procedures could be replaced by a model based on the real composite materials structure, this would represent progress. The basic understanding of light propagation and reflection mechanisms could be improved, and parametric studies for new material combinations would be possible, with some predictive power.

In this study, ILM methods were applied and combined with transmittance measurements. A transmission model based on the Fresnel reflection/refraction theory was developed to determine the RI of the delignified wood template. The obtained RI values are valuable references for transparent wood fabrication and for modelling of light propagation in wood based transparent composites. The method could be also applied to measure the RI of other types of porous or layered materials and composites.

Diffused porous wood, balsa and birch, were used as the raw materials and cut from longitudinal wood sections (left image in Fig. 2a). The sodium chlorite ( $\text{NaClO}_2$ , Sigma-Aldrich) based delignification process was used according to our previous work to remove light absorbing components (mainly lignin).<sup>10</sup> The delignified templates were dried under supercritical  $\text{CO}_2$  (Autosamdri-815, Tousimis, USA) in order to preserve the original structure of the wood templates, see Fig. 2a. The amount of residual lignin (Klason lignin) in delignified wood templates is 1.5% for delignified balsa and 2% for delignified birch, measured according to the TAPPI method.<sup>29</sup> Next, the delignified samples were immersed in different liquids (ethanol, VWR; 1,2,4-trichlorobenzene, Merck; hexadecane, toluene, anisole and 1,2-dichlorobenzene, Sigma-Aldrich) with different RIs (Table 1, measured with J457 Automatic Refractometer, Rudolph Research Analytical, USA), and infiltrated under

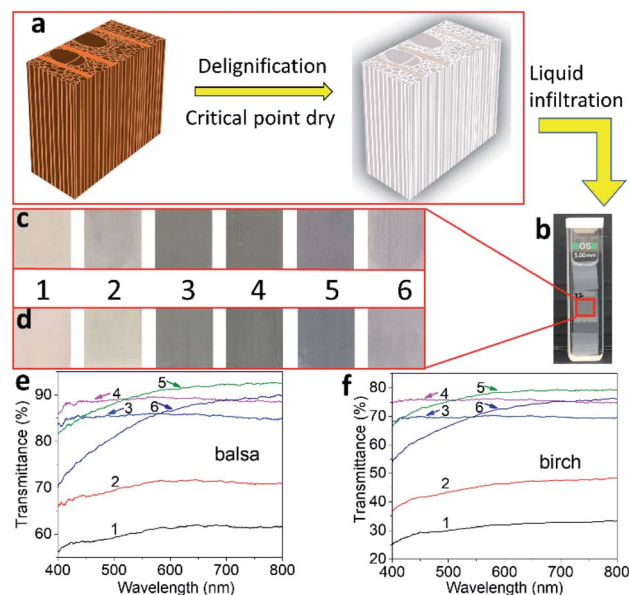


Fig. 2 (a) Preparation of delignified wood template, (b) delignified wood sample immersed in liquid inside the cuvette, delignified (c) balsa and (d) birch samples immersed in different liquids (see Table 1) showing difference in light transmission. Note the background is black. Transmittance spectra for (e) balsa and (f) birch samples immersed in six different liquids 1–6.



**Table 1** Refractive index of the liquids, measured at wavelength of 589 nm at 25 °C

| Liquid no. | Chemical name          | Refractive index |
|------------|------------------------|------------------|
| 1          | Ethanol                | 1.3596           |
| 2          | Hexadecane             | 1.4326           |
| 3          | Toluene                | 1.4939           |
| 4          | Anisole                | 1.5146           |
| 5          | 1,2-Dichlorobenzene    | 1.5493           |
| 6          | 1,2,4-Trichlorobenzene | 1.5695           |

vacuum for 7 days to ensure complete infiltration. The advantage of using different liquids instead of mixture of two liquids (the classic ILM) is to avoid the RI change during the vacuum treatment. For example, the RI of the mixture (ethanol + 1,2,4-trichlorobenzene) was changed from 1.537 to 1.566 after vacuum infiltration due to the different volatility of the separate components.

In order to ensure accurate and repeatable optical property measurements, the delignified wood sample was fixed in a specific sample holder designed for the purpose, then placed in the cuvettes (optical glass cuvette, pathlength = 5 mm, Sigma-Aldrich) as shown in Fig. 2b. Then all the cuvettes were filled with the liquids as shown in Table 1. Since the RIs and the birefringence of the fiber are influenced by temperature,<sup>30</sup> all the samples were heated to 25 °C for 4 hours in a water bath before the optical measurement. In Fig. 2c (delignified balsa) and 2d (delignified birch), the samples show a more transparent appearance when immersed in liquids no. 4 and no. 5 with a black background (in Table 1, samples immersed in different liquids are termed no. 1–6).

Angle-integrated transmittance of samples immersed in different liquids was measured with an integrating sphere according to ASTM D1003.<sup>31</sup> The sample was held in front of the input port of an integrating sphere. An unpolarized light source (quartz tungsten halogen light source, model 66181 from Oriel Instruments) served as the incident beam. The transmitted light was averaged by the integrating sphere and its intensity was measured by a spectrometer connected to an output port of the sphere through an optical fiber. Fig. 2e and 2f show the recorded spectra in the visible range for balsa and birch, respectively. It is clear that at the wavelength of 589 nm, the transmittances of balsa and birch samples are first gradually increased from liquid no. 1 to no. 5, and then decreased at liquid no. 6. This means that the RIs of the delignified wood templates are closer to liquid no. 5 for both wood species. At shorter wavelength (*i.e.* around 450 nm), however, the transmittance shows a different trend for both cases, where the transmittance of sample no. 5 is lower than for no. 4. The reason is that the RI of the delignified wood template depends strongly on the wavelength.<sup>16,19,23</sup> The exact values of the RI are, however, still unknown. A theoretical model is needed to fit the experimental data and to extract the RI.

In order to find the maximum transmittance of the samples, a transmission model based on Fresnel reflection/refraction for

planar waves was developed. The Fresnel equation describes the light reflection and refraction at the interface between two materials of different RIs.<sup>32</sup> In general, it is a function of the incoming angle, the refracted angle (Snell's law), refractive indices of the media, and the light polarization. The model is applicable to transparent wood, but also to other types of fiber composites.

We start from a simplified picture of the transverse surface represented as a number of planar interfaces (Fig. 3). Note that other fiber composites, for instance unidirectional glass fiber composites in a polymer matrix, could be represented in the same way. A proper treatment of such a multilayer structure requires to consider both phases and amplitudes of the propagating wave, in order to account for interference effects due to multiple reflections. It can be done by introducing a concept of "optical impedance", which allows analytical solutions for some geometries.<sup>33</sup> Here we note that the cell wall structure is corrugated on the order of several microns, thus averaging out possible constructive and destructive interference effects. Therefore, we limit our consideration to the amplitude part of the reflection. The transmitted light intensity will decrease due to the Fresnel reflection on each such interface with a coefficient  $R = \left(\frac{x-n}{x+n}\right)^2$ , where  $n$  is the refractive index of the delignified wood template, and  $x$  is the refractive index of a liquid. If there are  $N$  interfaces per unit length in the material as shown in Fig. 3a, we can introduce a continuous parameter  $\mu$ , which is a reflection coefficient:  $\mu = RN$ . Then the probability density of Fresnel reflection to occur at the length  $l$  is  $p(l) = \mu e^{-\mu l}$ . The probability of this event at the interval  $(l; l + dl)$  is  $p(l) dl$ . In order to calculate the probability of the total transmittance in this case, the Fresnel reflection loss should be calculated by integrating  $p(l)$  from 0 to  $d$  (sample thickness):

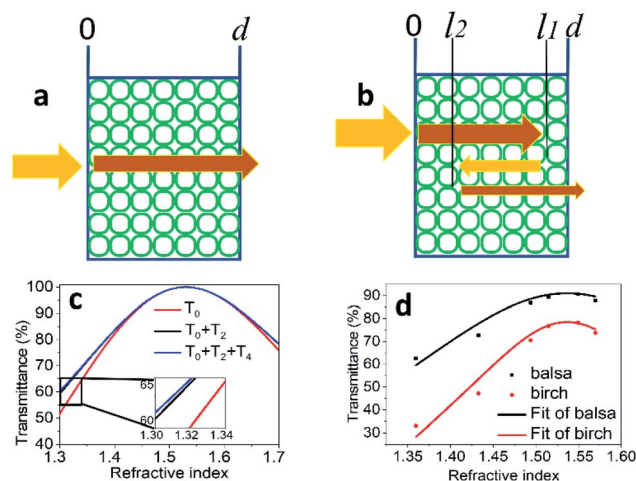


**Fig. 3** Transmission model for delignified wood template based on Fresnel reflection theory. The green "squares" are surrounding the lumen space of the delignified wood template, which is filled with liquid. With respect to beam reflection inside the material: (a) represents no reflection and (b) reflection 2 times. (c) Comparison between  $T_0$ ,  $T_0 + T_2$  and  $T_0 + T_2 + T_4$ . (d) Transmission model fit of the transmittance values at wavelength 589 nm for both delignified balsa and birch samples.





$$T_0 = 1 - R_{\text{loss}} = 1 - \int_0^d p(l)dl = e^{-\mu d} \quad (1)$$

This is a formula for the first passage, as shown in Fig. 3a (case 1): the beam goes through the material (with thickness  $d$ ) where reflection simply reduces the transmission. We can include multiple passages to the final formula as well. For example, in the case of two reflections, the beam propagation inside the sample can be separated into 3 stages (case 2) as shown in Fig. 3b. The beam first goes into the sample and it is reflected at the depth  $l_1$ . Then the beam reflects back at the point with depth  $l_2$ , travelling at this stage with optical path  $l_1 - l_2$ . Finally, the once again reflected beam escapes from the sample. The final stage is similar to case 1, so its transmittance probability can be written as  $e^{-\mu(d-l_2)}$ . The light propagation in this case experiences the Fresnel reflection at the end of intervals  $(0; l_1)$  and  $(l_1; l_2)$ . Summing up corresponding probability densities we obtain the transmittance in case 2:

$$T_2 = \int_0^d \int_0^{l_1} p(l_1)p(l_1 - l_2)e^{-\mu(d-l_2)} dl_2 dl_1 \quad (2)$$

$$= \frac{1}{4}(2\mu d - 1)e^{-\mu d} + \frac{1}{4}e^{-3\mu d}$$

Further multiple passage expressions can be derived in a similar way, although formulas become cumbersome (not shown).

Thus, the total transmittance will be the sum of all the multiple passages (only even numbers), which is  $T_{\text{total}} = T_0 + T_2 + T_4 + \dots$ . A comparison between  $T_0$ ,  $T_0 + T_2$  and  $T_0 + T_2 + T_4$  is shown in Fig. 3c, with a fixed value of the linear density of interfaces inside the sample  $N = 100$  and the RI of the tested sample  $n = 1.53$  (both values are relevant for present experiments). From Fig. 3c, a slight difference between  $T_0$  (the red curve) and  $T_0 + T_2$  (the black curve) is observed, while there is almost no difference between  $T_0 + T_2$  (the black curve) and  $T_0 + T_2 + T_4$  (the blue curve). This comparison shows that the contribution of the beam reflected 4 times to total transmittance here is very small and could be ignored. Therefore, a limiting description to  $T_0 + T_2$  is feasible for the total transmittance. Thus, combining eqn (1) and (2), one obtains:

$$T_{\text{total}} = \left( \frac{1}{2}N \left( \frac{x-n}{x+n} \right)^2 d + \frac{3}{4} \right) e^{-N \left( \frac{x-n}{x+n} \right)^2 d} + \frac{1}{4} e^{-3N \left( \frac{x-n}{x+n} \right)^2 d} \quad (3)$$

where  $T_{\text{total}}$  is the total transmittance,  $N$  is the linear density of the interfaces,  $n$  is the refractive index of the delignified wood template,  $x$  is the refractive index of the liquids, and  $d$  is the sample thickness. Finally, to account for small absorption losses (low lignin content) a pre-factor can be added. That is, for the highest transmittance probability (when  $x = n$ ), the value will not reach unity because of the light absorption inside the sample.

In order to find the RI of the delignified wood template, the transmittance (at wavelength of 589 nm) of all the samples was

fitted with eqn (3), as shown in Fig. 3d. When the transmittance reaches the maximum value, the corresponding value of  $x$  is assigned as the RI of the delignified wood template. From Fig. 3d, it is clear that the maximum value of total transmittance for all the samples does not reach 100%. Possible reasons include the inhomogeneous structure of the delignified wood templates with the associated light scattering, or that some light is absorbed by residual lignin in the wood template. The RI values perpendicular to the wood fibers obtained from the fitting are  $1.536 \pm 0.006$  and  $1.537 \pm 0.005$  for delignified balsa and birch, respectively. According to our model, the refractive index for the delignified wood template is a material property intrinsic to a particular wood template. The difference in MFA, chemical composition as well as swelling ability in the infiltrated liquids are possible reasons<sup>12–15</sup> for slight differences of the RIs between delignified balsa and birch templates. There is some difference between the values obtained in current work and in the literature,<sup>18,19,23,25,26</sup> mainly due to the complex wood structure included during the measurement in this work as well as the chemical composition difference.

The number of linear interfaces (LIs) can also be obtained from the fitting based on the transmission model, which is found to be 138 for balsa. We can compare this value with the experimental results from micrographs obtained with a field-emission scanning electron microscope (SEM, Hitachi S-4800, Japan) shown in Fig. 4a. From Fig. 4b, the average diameter of a single cell is around 30  $\mu\text{m}$ . The diameter of larger vessel cells ranged from 180 to 300  $\mu\text{m}$ . The linear density of cells per mm for balsa is between 30 and 40. In the light propagation direction, this corresponds to 120–160 interfaces, where each cell contributes with 4 interfaces: 2 cell wall/middle lamella interfaces (green arrow in Fig. 4c) and 2 cell wall/lumen interfaces (red arrow in Fig. 4c). For birch, the number of the interfaces per mm was 376, as extracted from the transmission model. This value is also compared with SEM micrographs in Fig. 4d. For birch, the average diameter of a single fiber cell is around 12  $\mu\text{m}$  as shown in Fig. 4e, and the vessel cells are between 50 to 100  $\mu\text{m}$ . The linear density of cells is between 80 and 100 per mm, corresponding to a number of interfaces between 320 and 400 for birch. Again, interfaces originate from the cell wall/middle lamella interface (green arrow in Fig. 4f) and cell wall/

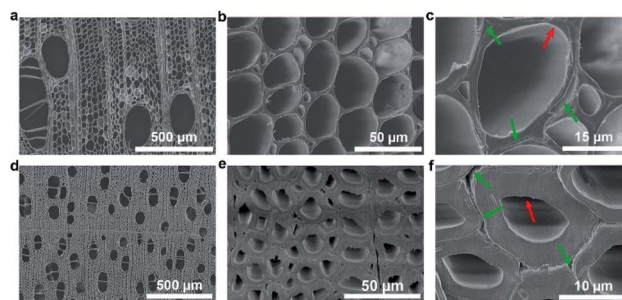


Fig. 4 FE-SEM micrographs at different scales of balsa (a), (b) and (c) and birch (d), (e) and (f), respectively. The green arrows point at cell wall/middle lamella interfaces, the red arrows indicate the cell wall/lumen interfaces.



lumen interface (red arrow in Fig. 4f). Considering the approximate nature of the model, the number of interfaces estimated from the transmission model is in very good agreement with the experimentally observed morphology in the direction normal to the specimen surface. We note that the cell walls surrounding lumens in nature with a shape close to circular instead of planar act as miniature lenses. As a result, most of the photons will be refracted, leading to a distribution of optical paths. Therefore, an average optical path value instead of the sample thickness should be used in eqn (3). Since the sample thickness here is relatively thin (1 mm), the sample thickness and the real average optical path could be approximated to be very close.

The maximum transmittance of the samples immersed in the liquids was also obtained from the model by fitting to the experimental data as shown in Table 2. In order to verify these values, the transmittance of the delignified balsa and birch immersed in the mixtures (RI = 1.536 and 1.537 for balsa and birch, respectively) was measured. The liquid mixtures were prepared with anisole (RI = 1.5146) and 1,2-dichlorobenzene (RI = 1.5493) from Table 1, using their weighted linear combination. The RI of the resulting solution was measured in a refractometer and it remained stable after vacuum treatment. The transmittance at wavelength 589 nm for delignified balsa and birch filled with these solutions are 91.1% and 78.5% (Table 2), which are in agree with the fitted results. This control experiment confirmed that the present model predicts reliable values both for the refractive index and the transmittance of the composite. Based on the success of the present model, the general mechanism for optical transmission in transparent wood composites from different polymers is expected to be the same, provided there are no additional "optical defects". The strong haze (light scattered forward at large angle) typically observed experimentally in transparent wood composites, is to a certain extent influenced by the mismatch in RI between the polymer and the wood cell wall material. The exact RI values determined here for the cell wall material, will make it possible to select polymers with more carefully matched RI, for better control of haze and transmittance characteristics.

Mathematical fittings, such as Lorentz, Gauss, and polynomial fittings were also performed to get the refractive index and the maximum transmittance of balsa and birch. The results show that there is no significant difference between these fittings. Our model is superior due to the match with experimental data and proper physical background which is lacking in the pure mathematical fittings. In particular, with the help of proposed model one can determine material-specific

parameters of the samples, such as a number of optical interfaces. This, in turn, makes possible to quantify variations in samples as a result of different preparation or treatment conditions.

In addition, the RIs parallel to wood fiber direction were also measured for delignified wood samples, and found to be  $1.525 \pm 0.008$  for balsa, and  $1.529 \pm 0.006$  for birch, respectively. In this case, however, the interfaces originate from ray cells extending in the radial direction of the tree stem, fiber-fiber end interfaces and imperfect alignment of the fibers in the longitudinal direction. Exact values for the number of interfaces per unit length could therefore not easily be determined experimentally.

## Conclusions

In summary, we successfully measured the transmittance of the delignified wood samples immersed in selected liquids (immersion liquid method). In addition, a transmission model based on the Fresnel reflection/refraction theory was developed to find the refractive indices of the delignified wood samples in two fiber directions. The main idea is to find the maximum transmittance of the sample immersed in different liquids with different refractive indices, and retrieve the refractive index of the delignified wood template by fitting the measured results to the theoretical curve. Here, on the basis of the fitting of transmittance, we obtained the refractive indices for the delignified balsa wood template in the perpendicular and parallel to the wood fiber directions, which are  $1.536 \pm 0.006$  and  $1.525 \pm 0.008$ , respectively, and  $1.537 \pm 0.005$  and  $1.529 \pm 0.006$  for delignified birch wood template, at the wavelength of 589 nm. By comparison with the theoretical model, it is found that the microscopic origin of reduced transmission is the reflection and refraction at the cell wall/lumen and cell wall/middle lamella interfaces. The obtained RIs of the delignified wood templates can be used in the design and fabrication of transparent wood composites, tuning the optical properties by infiltrating wood templates with polymers of selected refractive index, and also for modelling light propagation in the delignified wood-based transparent composites. It is also applicable to unidirectional glass fiber/polymer composites, since their morphology is similar to the geometrical model in Fig. 3. In addition, the immersion liquid method in combination with the transmission model developed here, can be also applied to measure the refractive index of other types of layered or porous materials and composites.

## Conflicts of interest

There are no conflicts to declare.

## Acknowledgements

This project has received funding from the European Research Council (ERC) under the European Union's Horizon 2020 research and innovation program (grant agreement no. 742733). We acknowledge funding from KTH and Knut and

**Table 2** The maximum transmittance of delignified balsa and birch samples obtained by fitting and measurement of the samples in mixture of anisole and 1,2-dichlorobenzene at wavelength of 589 nm

| Samples           | Fitted transmittance (%) | Measured transmittance (%) |
|-------------------|--------------------------|----------------------------|
| Delignified balsa | 90.9                     | 91.1                       |
| Delignified birch | 78.5                     | 78.5                       |



Alice Wallenberg foundation through the Wallenberg Wood Science Center at KTH Royal Institute of Technology. Adil Baitenov and Xuan Yang are acknowledged for the discussions.

## References

- 1 J. Gou, L. Song, H. Liu, D. Shen, W. Hu, W. Wang, X. Ren and J. Chang, *J. Bioresour. Bioprod.*, 2019, **4**, 166–176.
- 2 X. Yang, X. Tang, L. Ma and Y. Sun, *J. Bioresour. Bioprod.*, 2019, **4**, 111–118.
- 3 Y. Li, E. Vasileva, I. Sychugov, S. Popov and L. Berglund, *Adv. Opt. Mater.*, 2018, **6**, 1800059.
- 4 Y. Li, Q. Fu, X. Yang and L. Berglund, *Philos. Trans. R. Soc., A*, 2018, **376**, 20170182.
- 5 S. Iwamoto, A. N. Nakagaito, H. Yano and M. Nogi, *Appl. Phys. A*, 2005, **81**, 1109–1112.
- 6 S. Fink, *Holzforschung*, 1992, **46**, 403–408.
- 7 H. Chen, A. Baitenov, Y. Li, E. Vasileva, S. Popov, I. Sychugov, M. Yan and L. Berglund, *ACS Appl. Mater. Interfaces*, 2019, **11**, 35451–35457.
- 8 T. Keplinger, E. Cabane, J. K. Berg, J. S. Segmehl, P. Bock and I. Burgert, *Adv. Mater. Interfaces*, 2016, **3**, 1600233.
- 9 T. Nilsson and R. Rowell, *J. Cult. Herit.*, 2012, **13**, S5–S9.
- 10 Y. Li, Q. Fu, S. Yu, M. Yan and L. Berglund, *Biomacromolecules*, 2016, **17**, 1358–1364.
- 11 E. Vasileva, A. Baitenov, H. Chen, Y. Li, I. Sychugov, M. Yan, L. Berglund and S. Popov, *Opt. Lett.*, 2019, **44**, 2962–2965.
- 12 A. Frey, *Kolloidchem. Beih.*, 1926, **23**, 40–50.
- 13 M. Meyer and A. Frey-wyssling, *Helv. Chim. Acta*, 1935, **18**, 1428–1435.
- 14 K. Kisou, *Helv. Chim. Acta*, 1934, **17**, 1047–1066.
- 15 P. H. Hermans, J. J. Hermans and D. Vermaas, *J. Colloid Sci.*, 1946, **1**, 251–260.
- 16 R. C. Faust, *Proc. Phys. Soc.*, 1952, **65**, 48–62.
- 17 S. M. Ojena and P. R. De Forest, *J. Forensic Sci. Soc.*, 1972, **12**, 315–329.
- 18 I. Niskanen, J. Heikkinen, J. Mikkonen, A. Harju, H. Heräjärvi, M. Venäläinen and K. E. Peiponen, *J. Wood Sci.*, 2012, **58**, 46–50.
- 19 H. Juttula and A. J. Mäkyne, *2012 IEEE I2MTC – Int. Instrum. Meas. Technol. Conf. Proc.*, 2012, pp. 1231–1234.
- 20 D. J. O'Brien, B. Parquette, M. L. Hoey and J. Perry, *Polym. Compos.*, 2018, **39**, 2523–2534.
- 21 H. Contreras-Tello and A. García-Valenzuela, *Appl. Opt.*, 2014, **53**, 4768–4778.
- 22 W. R. Calhoun, H. Maeta, A. Combs, L. M. Bali and S. Bali, *Opt. Lett.*, 2010, **35**, 1224–1226.
- 23 G. M. Patel, *Die Makromol. Chemie*, 1951, **7**, 12–45.
- 24 R. Mosebach, *Z. Phys. Chem.*, 1954, **2**, 375–376.
- 25 K. R. K. Iyer, P. Neelakantan and T. Radhakrishnan, *J. Polym. Sci., Part A-2*, 1968, **6**, 1747–1758.
- 26 J. M. Preston, *Trans. Faraday Soc.*, 1933, **29**, 65–71.
- 27 I. Niskanen, T. Suopajärvi, H. Liimatainen, T. Fabritius, R. Heikkilä and G. Thungström, *J. Quant. Spectrosc. Radiat. Transfer*, 2019, **235**, 1–6.
- 28 R. J. Nussbaumer, M. Halter, T. Tervoort, W. R. Caseri and P. Smith, *J. Mater. Sci.*, 2005, **40**, 575–582.
- 29 Tappi Press, *Acid-insoluble lignin in wood and pulp, Tappi T 222 om-02, 2002–2003 TAPPI Test Methods*, 2002.
- 30 A. Frey-Wyssling and K. Wuhrmann, *Helv. Chim. Acta*, 1939, **22**, 981–988.
- 31 ASTM International, *Standard Test Method for Haze and Luminous Transmittance of Transparent Plastics*, ASTM D1003, 2003.
- 32 M. Born and E. Wolf, *Principles of Optics: Electromagnetic Theory of Propagation, Interference and diffraction of light*, 6th edn, Elsevier, Amsterdam, Netherlands, 2013.
- 33 L. Brekhovskikh, *Waves in Layered Media*, Elsevier, Amsterdam, Netherlands, 2012, vol. 16.

